

Embryonic Toxin Expression in the Cone Snail *Conus victoriae* *PRIMED TO KILL OR DIVERGENT FUNCTION?*^{*§}

Received for publication, December 30, 2010, and in revised form, March 28, 2011. Published, JBC Papers in Press, April 19, 2011, DOI 10.1074/jbc.M110.217703

Helena Safavi-Hemami^{†§}, William A. Siero[¶], Zhihe Kuang^{||}, Nicholas A. Williamson[§], John A. Karas[§], Louise R. Page^{**}, David MacMillan[¶], Brid Callaghan^{††}, Shiva Nag Kompella^{††}, David J. Adams^{††1}, Raymond S. Norton^{¶§§2}, and Anthony W. Purcell^{†§§3}

From the [†]Department of Biochemistry and Molecular Biology, [§]Bio21 Molecular Science and Biotechnology Institute, and [¶]Department of Zoology, University of Melbourne, 3010 Victoria, Australia, ^{||}The Walter and Eliza Hall Institute of Medical Research, Parkville, 3052 Victoria, Australia, the ^{**}Department of Biology, University of Victoria, Victoria, British Columbia V8W 3N5, Canada, the ^{††}Health Innovations Research Institute, RMIT University, Melbourne, 3083 Victoria, Australia, and the ^{§§}Medicinal Chemistry and Drug Action, Monash Institute of Pharmaceutical Sciences, Faculty of Pharmacy and Pharmaceutical Sciences, Monash University, Parkville, 3052 Victoria, Australia

Predatory marine cone snails (genus *Conus*) utilize complex venoms mainly composed of small peptide toxins that target voltage- and ligand-gated ion channels in their prey. Although the venoms of a number of cone snail species have been intensively profiled and functionally characterized, nothing is known about the initiation of venom expression at an early developmental stage. Here, we report on the expression of venom mRNA in embryos of *Conus victoriae* and the identification of novel α - and O-conotoxin sequences. Embryonic toxin mRNA expression is initiated well before differentiation of the venom gland, the organ of venom biosynthesis. Structural and functional studies revealed that the embryonic α -conotoxins exhibit the same basic three-dimensional structure as the most abundant adult toxin but significantly differ in their neurological targets. Based on these findings, we postulate that the venom repertoire of cone snails undergoes ontogenetic changes most likely reflecting differences in the biotic interactions of these animals with their prey, predators, or competitors. To our knowledge, this is the first study to show toxin mRNA transcripts in embryos, a finding that extends our understanding of the early onset of venom expression in animals and may suggest alternative functions of peptide toxins during development.

Cone snails of the genus *Conus* are predatory marine gastropods that utilize venom to capture prey. *Conus* venoms mainly consist of small disulfide-rich peptides commonly referred to as

conotoxins or conopeptides. Each of the ~700 *Conus* species synthesizes its own characteristic repertoire of toxic peptides. It has been estimated that the toxin repertoire of cone snails comprises >100,000 different bioactive compounds with various neurological targets (1). Remarkably, this vast library of bioactive peptides has been generated by a relatively small number of gene superfamilies (2, 3). Conotoxins are translated as precursor proteins with an N-terminal signal sequence, an intermediate pro-region followed by the mature toxin at the C terminus. Comparisons between the different gene superfamilies revealed high conservation within the primary amino acid sequence for the signal and pro-sequence, whereas the mature toxin region exhibits hypermutation between a conserved disulfide scaffold (2). The venom repertoire of cone snails is further extended through the addition of post-translational modifications that increase toxin potency (4, 5) and aid in stabilizing the three-dimensional structure of the molecule (6, 7). Such is the diversification of conotoxins that venom profiles differ significantly among individuals of the same species (8–10). The exact mechanism underlying the accelerated evolution of conotoxins is not yet understood, but it has been suggested that rapid genetic divergence is driven by the various interactions between the toxins and the snail's biotic environment. Besides their function in predation, anecdotal evidence points to the role for conotoxins in deterring predators and competitors (2, 11). Given the diversity of disulfide-rich peptides in *Conus*, other functions, such as regulation of social behavior as observed in other molluscs (12, 13), may exist in this genus.

Very little is known about the onset of venom synthesis in cone snails. Female cone snails typically lay their eggs in egg capsules attached to a benthic substrate. Prehatching time, hatching size, and total prejuvenile development greatly vary between different *Conus* species and depend to a large extent on the presence or absence of a feeding larval stage (14–17). The few studies addressing feeding behavior of juvenile snails indicate that predation can occur a few days after larval metamorphosis (18), suggesting initialization of venom biosynthesis at an earlier developmental stage. Although juveniles of *Conus textile* were shown to feed on the same prey as adults (18), specimens of *Conus magus* exhibited a change in prey type from polychaetes to fish as they matured

* This work was supported in part by Australian Research Council Grant DP110101331 (to A. W. P. and N. A. W.).

§ The on-line version of this article (available at <http://www.jbc.org>) contains supplemental Figs. 1–4 and Table 1.

The nucleotide sequence(s) reported in this paper has been submitted to the GenBank™/EBI Data Bank with accession number(s) GU046308, GU046309, JF433900, JF433901, JF433902, JF433903, JF433904, JF433905, JF433906, JF433907, JF433908, JF433909, JF433910.

¹ Professorial fellow of the Australian Research Council.

² Recipient of a National Health and Medical Research Council of Australia principal research fellowship.

³ Recipient of a National Health and Medical Research Council of Australia senior research fellowship. To whom correspondence should be addressed: Bio21 Molecular Science and Biotechnology Institute, 30 Flemington Rd., 3010 Victoria, Australia. Tel.: 61-3-8344-2288; Fax: 61-3-9348-141; E-mail: apurcell@unimelb.edu.au.

(19). Whether the venom composition changed during this transition was not determined.

Among the most extensively studied cone snail toxins are the α -conotoxins, known antagonists of the nicotinic acetylcholine receptors (nAChRs)⁴ (20–22). Recent studies have also identified N-type calcium channels as another neuronal target for a number of α -conotoxins (23, 24). α -Conotoxins inhibit these channels via activation of the GABA_B receptor (24) and target these receptors and ion channels with exquisite selectivity. Target specificity not only varies between toxins from different *Conus* species but, remarkably, even between peptides isolated from the same individual (25). It is likely that the expression profile of α -conotoxins exhibiting different target specificity reflects an adaptation to the biotic environment.

In this study, we demonstrate that prior to hatching, embryos of *Conus victoriae* are capable of expressing venom mRNA. Interestingly, embryonic α - and O-conotoxin sequences differ significantly from adult toxin transcripts. Embryonic α -conotoxins were chosen for further characterization. Although the novel embryonic α -conotoxin Vc1.2 shares the same three-dimensional structure of the previously reported adult toxin Vc1.1, these peptides exhibit different affinities for the GABA_B receptor/N-type Ca²⁺ channels and distinct subtype selectivities for the nAChR. Despite thorough electrophysiological investigations, the target receptor for a second embryonic toxin, Vc1.3, could not be determined, suggesting a novel target for this particular venom species. It appears that cone snails at different developmental stages differ in the relative abundance of their bioactive peptides potentially reflecting their particular ontogenetic stage.

EXPERIMENTAL PROCEDURES

Specimen Collection and Histological Preparation—Specimens of *C. victoriae* were collected from Broome, Western Australia, maintained in flow-through seawater tanks at 24 °C, and fed every 2 weeks with live specimens of *Austrocochlea* spp. Approximately 4 weeks post-collection, two specimens of *C. victoriae* laid egg capsules, each containing between 20 and 50 eggs derived from two independent matings. For histological preparations, adult snails were transferred to seawater containing 2% MgCl₂ for 4 h followed by overnight fixation in 4% paraformaldehyde/phosphate-buffered saline (PBS). Specimens were washed in water for 15 min, decalcified for 5 h in 5% formic acid, and stored in 70% ethanol until further processing. Embryos from two specimens of *C. victoriae* were removed from their egg capsules 18 days after egg deposition and fixed in 4% paraformaldehyde/PBS. Embryos were sequentially washed in PBS and embedded in 2% agarose/PBS preheated to 60 °C. Once set, the agarose blocks were stored in 70% ethanol until further processing. Adult snails and embryos were processed, sectioned (7 μ m), and stained with Mallory's trichrome stain (26) following routine histological procedures.

Conotoxin cDNA Isolation and Sequencing—Venom ducts were dissected and embryos collected from two adult speci-

mens of *C. victoriae* 18 days after egg deposition, immediately snap-frozen in liquid nitrogen, and stored at –80 °C. The two sets of embryos represent the progeny of two independent mating events. Frozen embryos and venom duct tissues were ground under liquid nitrogen. Total RNA was extracted using TRIzol reagent (Invitrogen), and DNase I was treated with Turbo DNase (Ambion). RNA extraction and DNase treatment were performed according to the manufacturer's instructions. Total RNA concentrations were determined using a spectrophotometer, and RNA integrity was verified by gel electrophoresis. cDNA was reverse-transcribed from 720 ng of DNase-treated RNA using the transcriptor high fidelity cDNA synthesis kit (Roche Applied Science). Primary reverse transcription PCRs (RT-PCR) were performed in volumes of 30 μ l containing 2 μ l of cDNA (60 ng), 0.3 μ l of TITANIUM TaqDNA polymerase (Clontech), 1 \times Advantage 2 PCR buffer (Clontech), 200 μ M of each deoxynucleotide triphosphate (dNTPs), and 0.2 μ M of forward and reverse oligonucleotides (supplemental Table 1). PCR cycle conditions were 1 cycle at 94 °C for 3 min and 30 cycles at 94 °C, 54 °C for 30 s and 72 °C for 30 s, and then 72 °C for 10 min. To rule out false amplification of genomic DNA, a negative control was performed using a reverse transcription reaction from which the enzyme reverse transcriptase was excluded. Nested PCRs were performed as described above except 2 μ l of the 1:5 diluted primary PCR was used as DNA template, and oligonucleotides were replaced with 0.2 μ M of nested oligonucleotides (supplemental Table 1), and the annealing temperature was reduced to 43 °C for 30 s. All PCR amplicons were analyzed by gel electrophoresis, cloned into pGEM-T plasmid vectors (Promega), and subsequently sequenced as described previously (27). All sequences analyzed in this study were deposited in GenBankTM (National Center for Biotechnology Information, National Library of Medicine, Bethesda). Nucleotide sequences were translated into the predicted amino acid residues, and comparative alignments of the protein and nucleotide sequences were performed using MAFFT E-INS-i sequence alignment by means of local pairwise alignment information (28). The putative signal peptides were predicted using SignalP software (29).

Peptide Synthesis—The embryonic peptides Vc1.2 and Vc1.3 were synthesized using Fmoc (*N*-(9-fluorenyl)methoxycarbonyl) solid-phase peptide chemistry (Liberty peptide synthesizer, CEM Corp.). Peptides were cleaved from the solid-phase resin with TFA/H₂O/triisopropylsilane/3,6-dioxo-1,8-octanedithiol (90:2.5:2.5:5) for 2 h. The crude peptides were isolated by ether precipitation, dissolved 30:70, v/v, in ACN/H₂O, lyophilized, and purified on a C18 column (5- μ m particle size, dimensions are 15 cm \times 4.6 mm, Discovery C18 column, Supelco Inc.) using an Agilent 1200 HPLC system (Agilent) with a linear gradient from 10 to 60% buffer B (99% ACN, 0.1% TFA; buffer A, 0.1% TFA) over 30 min. The purified linear peptides were oxidized in 100 mM NH₄HCO₃ in water/ACN (v/v, 90:10%) at a concentration of 0.5 mg/ml for 16 h at room temperature. Oxidized peptides were isolated to a final purity of >94% on a C18 column (5- μ m particle size, dimensions: 9.4 cm \times 2.5 mm, Eclipse C18 column, Agilent) using an Agilent 1100 HPLC system with the gradient described above. The identities of the fully oxidized peptides were confirmed by high resolution mass

⁴The abbreviations used are: nAChR, nicotinic acetylcholine receptor; ACN, acetonitrile; HVA, high voltage-activated; DRG, dorsal root ganglion; ACh, acetylcholine.

Embryonic Toxin Expression in Marine Cone Snails

spectrometry (6510 Q-TOF LC/MS mass spectrometer, Agilent).

Electrophysiological Studies on Embryonic Peptides—RNA preparation, oocyte preparation, and expression of nAChR subunits in *Xenopus* oocytes were performed as described previously (30). Briefly, plasmids with cDNA encoding the rat $\alpha 3$, $\alpha 4$, $\alpha 9$, $\alpha 10$, $\beta 2$, and $\beta 4$ nAChR and human $\alpha 7$ subunits were subcloned into the oocyte expression vector pNKS2 and were used for mRNA preparation using mMMESSAGE mMACHINE kit (Ambion Inc.). All oocytes were injected with 5 ng of cRNA and then kept at 18 °C in ND96 buffer (96 mM NaCl, 2 mM KCl, 1 mM CaCl₂, 1 mM MgCl₂, and 5 mM HEPES, pH 7.4) supplemented with 50 mg/liter gentamycin and 5 mM pyruvic acid 2–5 days before recording. Membrane currents were recorded from *Xenopus* oocytes using an automated work station with eight channels in parallel, including drug delivery and on-line analysis (OpusXpress 6000A work station; Molecular Devices Inc.) and a two-electrode virtual ground voltage clamp circuit with a GeneClamp 500B amplifier (Molecular Devices). Both the voltage recording and current injecting electrodes were pulled from borosilicate glass (GC150T-15, Harvard Apparatus Ltd.) and had resistances of 0.2–1.5 megohms when filled with 3 M KCl. All recordings were conducted at room temperature (20–23 °C) using a bath solution of ND96 as described above. During recordings, the oocytes were perfused continuously at a rate of 1.5 ml/min, with 300-s incubation times for the conotoxin. Acetylcholine (100 mM for $\alpha 7$, 30 mM for all other nAChR subtypes) was applied for 2 s at 5 ml/min, with 300-s washout periods between applications. Cells were voltage-clamped at a holding potential of –80 mV. Data were sampled at 500 Hz and filtered at 50 Hz. Peak current amplitude was measured before and following incubation of the peptide (31).

Concentration-response curves for antagonists were fitted by unweighted nonlinear regression to the logistic equation, $E_x = E_{\max} X^{nH} / (X^{nH} + IC_{50}^{nH})$, where E_x is the response; X is the antagonist concentration; E_{\max} is the maximal response, nH is the slope factor, and IC_{50} is the concentration of antagonist that inhibits the agonist response by 50%. All electrophysiological data were pooled ($n = 4–8$ for each data point) and represent the means \pm S.E. of the fit. Computation was carried out using SigmaPlot 11.0 (Systat Software).

Dorsal root ganglion (DRG) neurons were enzymatically dissociated from ganglia of 7–14-day-old Wistar rats according to standard protocols as described previously (24). The external recording solution contained 150 mM tetraethylammonium chloride, 2 mM BaCl₂, 10 mM D-glucose, 10 mM HEPES, pH 7.3–7.4. Patch recording electrodes were filled with an internal solution containing 140 mM CsCl, 1 mM MgCl₂, 5 mM MgATP, 0.1 mM NaGTP, 5 mM 1,2-bis(2-aminophenoxy)ethane-*N,N,N',N'*-tetraacetic acid-Cs₄, 10 mM HEPES, pH 7.3, with CsOH and had resistances of 1.0–2.5 megohms. Membrane currents were recorded using the whole-cell configuration of the patch clamp technique with an Axopatch 200B amplifier (Molecular Devices). A voltage protocol using step depolarizations from –80 to –10 mV was applied when examining high voltage-activated (HVA) calcium channel currents with Ba²⁺ as

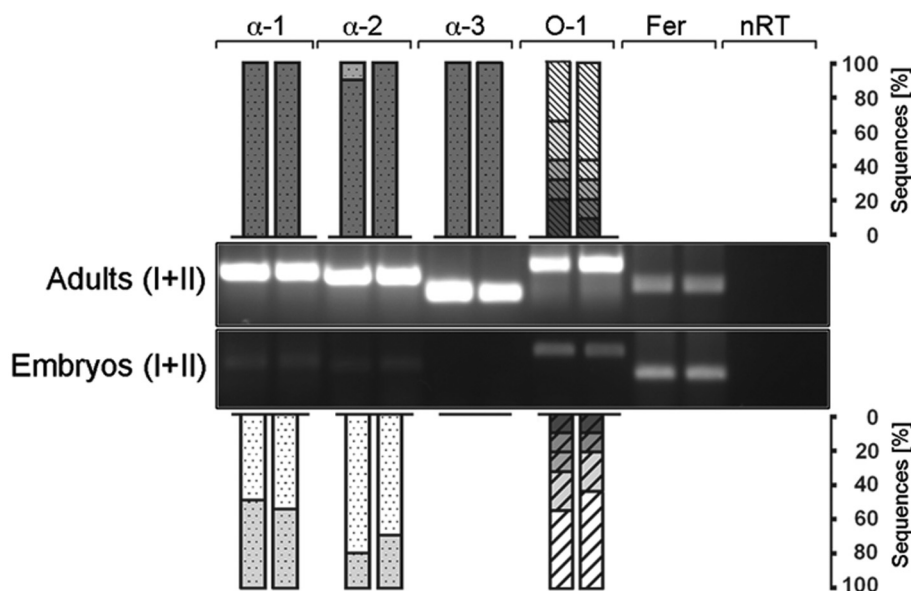
the charge carrier. Test potentials 150 ms in duration were applied every 20 s. Leak and capacitive currents were subtracted using a –P/4 pulse protocol. Membrane currents were acquired by a computer using pClamp 9.2 software (Molecular Devices), filtered at 2 kHz, and sampled at 8 kHz by the Digidata 1322A (Molecular Devices). Sampled data were stored digitally on a computer for further analysis.

NMR Spectroscopy and Structure Calculations—NMR experiments were performed at 25 °C on a 1.5 mM Vc1.2 sample in 95% H₂O, 5% ²H₂O, pH 3.6. Two-dimensional homonuclear TOCSY spectra, with a spin-lock time of 70 ms, and double quantum filtered correlated spectroscopy spectra were acquired on a DRX-600 spectrometer equipped with a triple resonance probe. Two-dimensional NOESY spectra with a mixing time of 250 ms, ¹⁵N HSQC, and ¹³C HSQC spectra were recorded on an Avance-800 spectrometer equipped with a TCI cryoprobe. Spectra were processed using TOPSPIN version 1.3 (Bruker Biospin Pty. Ltd.) and analyzed using XEASY (32). Backbone and side chain ¹H, ¹³C, and ¹⁵N chemical shifts were assigned. NOEs were assigned automatically using CYANA 2.1 (33, 34). The f and y angle constraints were predicted using TALOS⁺ (35) based on chemical shifts and were used in structure calculations when the predictions were consistent with an analysis of ³J_{H_NH _{α} coupling constants based on double quantum filtered-COSY spectra.}

A family of 200 structures was calculated using Xplor-NIH (36) using standard simulation annealing scripts. The 80 lowest energy structures were then subject to energy minimization in water; during this process, a box of water with a periodic boundary of 18.856 Å was built around the peptide structure, and the ensemble was energy-minimized on the basis of NOE and dihedral constraints and the geometry of the bonds, angles, and impropers (37). From this set of structures, a final family of 20 lowest energy structures was chosen for analysis using PROCHK-NMR (38) and MOLMOL (39). The final structures had no experimental distance violations greater than 0.2 Å or dihedral angle violations greater than 5°. The final structures and the associated structural constraints have been deposited in the BioMagResBank (40) under accession number 20126.

Protein Extraction and Mass Spectrometric Analyses—Venom ducts were dissected from four snails, and crude venom was manually squeezed from the ducts and air-dried. Approximately 1 mg of venom was reconstituted in 1 ml of ice-cold 30% ACN, 0.3% trifluoroacetic acid (TFA) followed by sonication for 10 min on ice. The extracts were centrifuged at 13,000 \times g for 20 min; the supernatants were lyophilized and reconstituted in 500 μ l of ultrapure water. Because of the complexity of the venom samples, extracts were separated by reversed-phase HPLC on a micropreparative C18 column (3.5 μ m particle size, dimensions: 2.1 \times 100 mm, X-Bridge, Waters) prior to mass spectrometric analysis using a linear gradient from 10 to 60% buffer B (95% ACN, 0.1% TFA; buffer A, 0.1% TFA) over 70 min. Reversed-phase venom fractions were individually analyzed on a MALDI-TOF mass spectrometer (QSTAR Pulsar, positive reflector mode, AB SCIEX). In addition to MALDI-TOF MS, venom extracts were analyzed by electrospray ionization-MS/MS. Samples were loaded onto a C18 reversed-phase column

A



B

Origin	Name	Sequence	Spacer	Toxin
α-1				
Adult (5+5)	Vc1.1	<u>MGMRMFTVFLSVVLATTVVSSTSG</u>	RREFRGRNAAAKASDLVSLTDKRR	GCCSDPRCNYDHPEICG
Embryo (6+6)	Vc1.2	<u>MGMRMFTVFLVLLVLTATTVVS</u>	FTSDRASDGRKAAASDLITLTIK	GCCSNPACMVNPNQICGRRR
Embryo (6+4)	Vc1.3	<u>MGMRMFTVFLVLLVLTATTVVS</u>	FTSDRASDGRKAAASDLITLTIK	GCCSDPPCIANNPDLGRRR
α-2				
Adult (6+7)	Vc1.1	<u>MGMRMFTVFLSVVLATTVVSSTSG</u>	RREFRGRNAAAKASDLVSLTDKRR	GCCSDPRCNYDHPEICG
Adult (1+0)	Vc1.1*	<u>MGMRMFTVFLSVVLATTVVSSTSG</u>	RREFRGRNAAAKASDLVSLTDKRR	GCCSDPRCNYDHSEICG
Embryo (4+6)	Vc1.2	<u>MGMRMFTVFLVLLVLTATTVVS</u>	FTSDRASDGRKAAASDLITLTIK	GCCSNPACMVNPNQICGRRR
Embryo (1+2)	Vc1.3	<u>MGMRMFTVFLVLLVLTATTVVS</u>	FTSDRASDGRKAAASDLITLTIK	GCCSDPPCIANNPDLGRRR
α-3				
Adult (5+5)	Vc1.1	-----	----- AAKASDLVSLTDKRR	GCCSDPRCNYDHPEICG
O-1				
Adult (2+1)	Vc6.7	<u>MEKLTILLVAAVLMSTQA</u>	VNQEKHQRKAKMNLSSKRKPPAERWWR	WGGCMAWFGLCSKDSECCSNSCDVTRCELMFPFPDW
Adult (0+1)	Vc6.8	<u>MEKLTILLVAAVLMSTQA</u>	LMQEQRQKAKINLFSKR	LSAESWWEENGCSLWGPCTVNAECCSGDCDETCIFGS
Adult (0+1)	Vc6.9	<u>MEKLTILLVAAVLMSTQA</u>	LMQEQRQKAKINLFSKRKPSAERR	WVDVGTCTFLGCTADAECSDNCVETVYCDLWW
Adult (1+0)	Vc6.10	<u>MEKLTILLVAAVLTSTQA</u>	LIQGGADERQKAKINLFSRSDR	ECRGYNAPCSAGAPCCSWWTCSTQTSRCE
Adult (2+1)	Vc6.11	<u>MEKLTILLVAAVLMSTQA</u>	LIQEQRQKAKINLFSKRKPSAER	WWGENDCRVFGSCTADEECCFNNCVQAYCFEV
Adult (4+5)	Vc6.12	<u>MQKLIIILLVAAVLMSTQA</u>	LFQEKRPMKKNLFSKGTDAEKQRKR	SCSDDWQYCEYPHDCSSWSCDVVCS
Embryo (1+1)	Vc6.13	<u>MEKLTILLVAAVLMSTQA</u>	LNQEQRQKAKINLSSKRKAPAERWWR	WGGCLLWFGRCMKDSECCSDSCDRTYCELARFPEGW
Embryo (1+1)	Vc6.14	<u>MEKLTILLVAAVLMSTQA</u>	MFQGGGKRPKDKIKFLSKRK	TNAESWWEGECLGWSNGTQPSDCCSNNCKGRNCDIW
Embryo (1+0)	Vc6.15	<u>MEKLTILLHVAAVLMSTQA</u>	LIQEQRQKAKINLFSKRKPSAER	WWGDNGCSLWGSCTVDAECCLGNCGGMYCSLLR
Embryo (1+2)	Vc6.16	<u>MQKLIIILLVAAVLMSTQA</u>	LFQEKRPKKIDLLSKRKTDAEKQQR	YCSDDSQPCHSHFYDCCWCSNNGYCP
Embryo (4+5)	Vc6.17	<u>MQELIIILLVAAVLMSTQA</u>	LFQEKRKKEKIDLLSKRKTDAEKQHR	LCPDYTDPCSNAYECCSWNCHNGHCTG

FIGURE 1. A, universal α - and O-conotoxin RT-PCR showing toxin mRNA expression in embryos ($n = 2$, each pooled from ~ 50 embryos) and adult specimens ($n = 2$) of *C. victoriae*. 110 ng of cDNA was amplified using three α - (α -1, α -2, and α -3) and one O-conotoxin (O-1) oligonucleotide pair. Ferritin (*Fer*) served as a reference gene. No reverse transcriptase controls (*nRT*) were performed to rule out contamination by genomic DNA. RT-PCRs were subsequently cloned and subjected to nucleotide sequencing. Bars represent the number of clones identified per RT-PCR expressed as percentages. DNA ladder: 1 kb plus (Invitrogen). *, analogue of Vc1.1 carrying one amino acid substitution. B, conotoxin sequences identified by RT-PCR showing the predicted signal peptide sequences (underlined), the spacer region, and the mature toxin region highlighted in gray. The number of clones sequenced per replicate ($n = 2$) is given in parentheses (43). GenBankTM accession numbers are as follows: Vc1.2, GU046308; Vc1.3, GU046309; Vc6.7, JF433900; Vc6.8, JF433901; Vc6.9, JF433902; Vc6.10, JF433903; Vc6.11, JF433904; Vc6.12, JF433905; Vc6.13, JF433906; Vc6.14, JF433907; Vc6.15, JF433908; Vc6.16, JF433909; and Vc6.17, JF433910.

(ProtoCol nano column, particle size 300 Å and 3 μ m, dimensions 75 μ m \times 100 mm, SGE Analytical Sciences) and analyzed using a Hybrid Quadrupole-TOF LC/MS/MS mass spectrometer (QSTAR Elite, AB SCIEX). Solvent A contained 0.1% formic acid, and solvent B consisted of 95% ACN, 0.1% formic acid. Separation was performed with a solvent B gradient of 5–60% over 90 min, followed by 60–80% B over 10 min. Acquired data were analyzed manually using Analyst QS software (version 2.0, AB SCIEX) accounting for the presence of various post-translationally modified peptide precursors (e.g. sulfation of tyrosines, γ -carboxylation

of glutamate, hydroxylation of proline, and C-terminal amidation).

RESULTS

Identification of Novel Conotoxin Transcripts in C. victoriae Embryos—RT-PCR using universal α - (41–43) and O-conotoxin (44) oligonucleotides led to the discovery of a number of novel toxin mRNA transcripts expressed in embryos and adults of *C. victoriae* and confirmed the presence of α -conotoxin Vc1.1 mRNA in the venom duct of adult specimens (Fig. 1) (43). All novel sequences were named according to the nomencla-

Embryonic Toxin Expression in Marine Cone Snails

A

```
C.victoriae_Vc1.2  MGMRMMFTVFLVVLATTVVSFTSD-RASDGRKAA---ASDLITLTIK--GCCSNPACMVNNPQICGRRR
C.victoriae_Vc1.3  MGMRMMFTVFLVVLATTVVSFTSD-RASDGRKAA---ASDLITLTIK--GCCSDPPCIANNPDLGRRR
C.pennaceus_Pn1B  MGMRMMFTVFLVVLATTVVSFTSD-RASDDGNAA---ASDLIALTIK--GCCSLPPCALSNPDYCG---
C.miles_Mil1.1    MGMRMMFTVFLVVLATTVVSFTSD-RGSDGRNAAAKDKASDLVALTVK--GCCSNPPCYANNQAYCNGRR
C.marmoratus_Mr1.1  MGMRMMFTMCLLVVLAATTVISFTSD-RASNGRNAAAKDKASDLNALNVR--GCCSHPACRVHYPHVCYGRR
C.litteratus_Lt1.1  MGMRMMFTMFLMLVVLATTVVFTSD-RALDAMNAAASNKASRLIALAVR--GCCARAACAGIHQELCGGGR
C.gercinus_QC1.4   MGMRMMFTVFLVVLATTV---TSD-RVSNGRKAAAKLKAPALMELSVRQ--GCCSDPACAVSNPDICGGGR
C.victoriae_Vc1.1  MGMRMMFTVFLVVLATTVVSSTSGRREFRGRNAAA--KASDLVSLTDKRGCCSDPRCNVDHPEICG---
C.textile_Tx1     MGMRMMFVFLVVLASTVVSSTSGRRFAHGRNAAA--KASGLVSLTDRRPECCSDPRCNSSHPELCCGGRR
C.textile_Tx2     MGMRMMFTVFLVVLATTVVSFTSGRRTFHGRNAAA--KASGLVSLTDRRPECCSHPACNVDPHEIC---R
***** : :*****:** ** * :** * . * * : ** : . * *
```

B

```
C.textile_TeA53-like  MQKLTILLVAAVLMSTQALNQ---EQHQKAKINLLSKRKPPAERWWRWGGCMLWFGRCTKDSECCSN-SCDRTYCELARFPPSDW
C.victoriae_Vc6.13  MEKLTILLVAAVLMSTQALNQ---EQHQKAKINLLSKRKAPAERWWRWGGCLLWFGRCTKDSECCSD-SCDRTYCELARFPEGW
C.victoriae_Vc6.7   MEKLTILLVAAVLMSTQAVNQ---EKHQKAKMNLSSKRKPPEERWWRWGGCMAWFGLCSDKSECCSN-SCDVTRCELMFPPPDW
C.victoriae_Vc6.8   MEKLTILLVAAVLMSTQALMQ---EQRQKAKINLFSKRRLSAESWWEENGCS-LWGPTVNAECCSG-DCDET-CIFG-----S
C.victoriae_Vc6.11  MEKLTILLVAAVLMSTQALIQ---EQRQKAKINLFSKRRKPSAERWWGENDCR-VFGSTAEDECCFN-NCVQAYCFEY----V
C.victoriae_Vc6.15  MEKLTILLHVAAVLMSTQALIQ---EQRQKAKINLFSKRRKPSAERWWDNGCS-LWGSCTVDABECCLG-NCGMYCSLL-----R
C.victoriae_Vc6.9   MEKLTILLVAAVLMSTQALMQ---EQRQKAKINLFSKRRKPSAERWVDVGCTFLLGCTADABECCSD-NCVETYCDLW-----W
C.litteratus_lt7b   MEKLTILLVAAVLMSTQALIQ---EKRQKAKITIFSKRKSNAERWWEGDCTDWLGSCSSPSECCYD-NCE-TYCTLW-----K
C.ventricosus_AAG60433  MEKLTILLVAAVLMSTQALIQ---EKRPKEKINLFSKRRKSIAESWWE-GECSGWSVHCTQHSDCCSG-ECTGSYCELY----V
C.tetulinus_Q3YEF9  MEKLTILLVAAVLMSTQALIQSDGEKRQQAKINFLSXRKSTAESWWE-GECKGWSVYCSWDNECCSG-ECTRYYCELW-----
C.victoriae_Vc6.14  MEKLTILLVAAVLMSTQAMFQGGEKRPKDKIFLSKRKTNAESWWE-GECLGWSNGCTQPSDCCSN-NCKGRNCDIW-----
C.textile_Gla(2)TxVI/B MEKLI ILLVAAVLMSTQALFQ---EKRTMKIDFLSKGKADAEKQRK-RNCSDDWQYCESPDCCSW-DCD-VVCS-----G
C.victoriae_Vc6.12  MQKLI ILLVAAVLMSTQALFQ---EKRPMKIFLSKGKTDAEKQRK-RSCSDDWQYCEPHDCCSW-SCD-VVCS-----
C.pennaceus_PnMEKL-032 MEKLI ILLVAAVLMSTQALFQ---EKRLEKIFLSKEKADAEKQQK-RYCSDQWKSCSYPHECCRW-SCN-RYCA-----
C.textile_Gla(3)TxVI MQKLI ILLVAAVLMSTQAVLQ---EKRPKEKIFLSKRKTDAEKQQK-RLCPDYTDPCSHAHECCSW-NCYNGHCT-----G
C.victoriae_Vc6.17  MQKLI ILLVAAVLMSTQALFQ---EKRREKIDLLSKRKTDAEKQHK-RLCPDYTDPCSNAYECCSW-NCHNGHCT-----G
C.victoriae_Vc6.16  MQKLI ILLVAAVLMSTQALFQ---EKRPKEIDLLSKRKTDAEKQQK-RYCSDSDSQPCSHFYDCCKW-SCNGYCP-----
C.textile_AAG60456  MEKLTILLVAAVLTSTQALIQGGDERQAKINFLSRSD-----RDCRGYDAPCSSGAPCDDWTCSARTNRCF-----
C.victoriae_Vc6.10  MEKLTILLVAAVLTSTQALIQGGDERQAKINFLSRSD-----RECRGYNAPCSGAPCCSSWTCSTQTSRCF-----
*:** *** ***:* * * : * : : : * : : : * * * *
```

FIGURE 2. Comparative alignment of novel embryonic α - (A) and O-conotoxins (B) isolated from *C. victoriae* with toxin sequences from other cone snail species. Alignment was performed using MAFFT E-INS-i sequence alignment by means of local pairwise alignment information (28). Sequences obtained from *C. victoriae* embryos and adults are highlighted *blue* and *orange*, respectively. Predicted protein signal sequences are *underlined* (SignalP). Conserved cysteine residues are shown in *boldface*, and the predicted mature toxin regions are highlighted *gray* (50). Basic and acidic amino acids are shown in *blue* and *red*, respectively. Dashes denote gaps. Amino acid conservations are denoted by an *asterisk*, and *colons* and *periods* represent a high and low degree of similarity, respectively.

ture previously used for *C. victoriae* venom peptides, where the first two letters indicate the species, the following number (1 or 6) represents the toxin family (α or O), and the last number implies the order of toxin discovery (e.g. Vc1.2 is the second α -conotoxin identified for *C. victoriae*) (45).

A total of five adult-specific and six embryo-specific O-superfamily toxins were identified, with no sequence overlap between these two life stages (Fig. 1B). Interestingly, the O-conotoxin expression pattern was nearly identical between the two sets of embryos tested with the exception of Vc6.15 which was only identified in one set of embryos (Fig. 1B). The most abundant transcript was Vc6.12 (47% of cloned sequences) in adults and Vc6.17 (54%) in embryos. O-superfamily toxins exhibit a characteristic pattern of 6 cysteines (C-C-CC-C-C) that form three disulfide bonds. Members of this family are known modulators of voltage-sensitive calcium, potassium, and sodium channels (44, 46). Alignment of the novel O-conotoxins with other members of the O-superfamily revealed high sequence similarity to the O2 gene superfamily (Fig. 2B), peptides with an as yet unidentified target receptor (44, 47).

Universal α -conotoxin RT-PCR identified two novel transcripts in the embryos (Vc1.2 and Vc1.3; Fig. 1) and confirmed the presence of Vc1.1 in the adults (43). Interestingly, utilizing a number of different universal α -conotoxin oligonucleotides

(α -1, α -2, and α -3; Fig. 1) did not lead to the identification of additional sequences suggesting that these toxins represent the most abundant α -conotoxin transcripts. In the adult, all but one clone (Vc1.1*) represented Vc1.1 (Fig. 1B). This finding is consistent with previous studies addressing α -conotoxin expression in *C. victoriae* (43, 45). The two cDNA transcripts identified from the embryos were almost equally represented with 55% for Vc1.2 and 45% for Vc1.3 using the α -1 oligonucleotide and slightly higher percentages for Vc1.2 (75%) when using the α -2 oligonucleotide (Fig. 1). The frequency of sequences obtained by RT-PCR screening generally indicates relative abundances of mRNA transcripts (48, 49). Thus, based on the number of clones obtained by primary RT-PCR analyses, relative abundances of toxin mRNAs varied greatly between the two life stages tested. The presence of such a limited yet distinct number of α -conotoxin transcripts was intriguing and was therefore further investigated.

*Embryonic and Adult α -Conotoxin Repertoire of *C. victoriae**—To further investigate α -conotoxin expression in adult *versus* embryos, toxin-specific oligonucleotides were designed for Vc1.1 and Vc1.2 (supplemental Table 1). Sequence similarities among the three transcripts precluded the design of specific PCR oligonucleotides for Vc1.3. Nested PCR can be utilized to detect low abundant transcripts and was performed on primary α -conotoxin PCRs using internal toxin-specific oligonucleo-

tides. Amplicons were successfully generated demonstrating that embryos express mRNA encoding the adult toxin Vc1.1 and that adults possess mRNA for the embryonic toxin Vc1.2 (supplemental Fig. 1).

Sequence Alignment of Novel Embryonic Toxins—Alignment of the novel embryonic toxin peptides with available α -conotoxin sequences revealed high similarity of the novel peptides to α -conotoxins sharing the conserved 4/7 cysteine pattern with 4 residues between C₁ and C₂, and 7 residues between C₃ and C₄ (Fig. 2). The predicted signal sequences and pro-regions share 100% identity although differences in the mature toxin regions are apparent. Based on observations made for other conotoxins, further proteolytic C-terminal cleavage and subsequent amidation of -CGRRR- to -C-NH₂- are likely to occur (50). Interestingly, protein alignment revealed the highest similarity of the pro-region and the mature toxin region between the embryonic peptides and α -conotoxin PnIB from *Conus pennaceus*, a potent inhibitor of the $\alpha 7$ subtype of the nAChR (51), although the adult toxin Vc1.1 is a known antagonist of the $\alpha 9\alpha 10$ subtype (52). To further elucidate potential differences in the neuronal target, electrophysiology was performed.

Determination of the Neuronal Target Receptor—The effects of Vc1.2 and Vc1.3 were examined on ACh-evoked currents mediated by various nAChR subtypes expressed in *Xenopus* oocytes. ACh (30–100 nM) was applied at 5-min intervals, and the peak amplitude of the corresponding membrane current was assessed. The peptide was applied 5 min prior to co-application of ACh plus peptide. Vc1.2 (1 nM) completely inhibited ACh-evoked currents mediated by $\alpha 3\beta 2$ nAChRs and inhibited the ACh-evoked current amplitude mediated by $\alpha 7$ and $\alpha 9\alpha 10$ nAChRs by 54 ± 5 and $46 \pm 4\%$ ($n = 3-5$), respectively (Fig. 3A). In contrast, Vc1.2 did not inhibit the $\alpha 3\beta 4$, $\alpha 4\beta 2$, or $\alpha 4\beta 4$ nAChR subtypes ($n = 3-5$) (Fig. 3A). Vc1.3 (1 nM) exhibited no significant activity at any of the neuronal nAChR subtypes (Fig. 3A). Concentration-response curves obtained for Vc1.2 displayed the following order of selectivity and corresponding IC₅₀ values: $\alpha 3\beta 2$ (75 ± 5 nM) > $\alpha 7$ (637 ± 90 nM) > $\alpha 9\alpha 10$ (~ 1 nM) (Fig. 3, B and E). These data indicate that Vc1.2 selectively and potently targets the $\alpha 3\beta 2$ and to a lesser extent the $\alpha 7$ nAChR subtype. The embryonic toxin Vc1.2 therefore exhibits a distinct nAChR selectivity to the adult toxin Vc1.1 (Fig. 3E).

Vc1.1 has previously been shown to inhibit N-type (Ca_v2.2) Ca²⁺ channel currents via activation of the G protein-coupled GABA_B receptor in sensory neurons (24). Therefore, the activity of Vc1.2 and Vc1.3 was also examined on depolarization-activated whole-cell Ba²⁺ currents in rat DRG neurons. Application of Vc1.2 inhibited HVA Ca²⁺ channel currents by 30.3% at 100 nM ($n = 9$) (Fig. 3, C–E). Vc1.3 was not active at 100 nM and inhibited the Ba²⁺ current amplitude by <20% at 1 μ M ($n = 7$) (Fig. 3, C–E). Both embryonic peptides Vc1.2 and Vc1.3 exhibit a reduced potency for GABA_B receptor-mediated inhibition of HVA Ca²⁺ channel currents compared with Vc1.1 (Fig. 3E).

Structure Determination of Vc1.2—To investigate whether subtype selectivity for the nAChR and affinity toward the GABA_B receptor arise from a difference in the three-dimensional structures of the peptides, the solution structure of Vc1.2 was determined using nuclear magnetic resonance (NMR)

spectroscopy. As can be seen in the one-dimensional ¹H NMR spectra recorded at different pH values and temperatures (supplemental Fig. 2), the backbone amide proton peak of Cys² was visible at pH 3.2 but not at pH 5.5 because of the exchange of solvent water; other peaks did not shift appreciably over the pH range 3.2–5.5, consistent with the fact that Vc1.2 does not contain charged residues and indicating that the structure is maintained over this pH range. A summary of experimental constraints and structural statistics for Vc1.2 is given in Table 1. The final 20 structures (Fig. 4A) fit well with experimentally derived distance and angle constraints and are well defined over the entire length of the polypeptide. The closest-to-average structure of Vc1.2 (Fig. 4B) is characterized by an α -helix (residues 6–11), as was also seen in other α -conotoxins with the same loop I and loop II lengths, such as Vc1.1 (30) and PnIA (53). The N-terminal residues 2–4 also appear to form a ₃₁₀ helix-like turn structure. The *trans* orientations of the peptide bond preceding both Pro⁶ and Pro³ were established by the intense H ^{α} –H ^{δ} nuclear Overhauser effects (NOEs) between the prolines and their preceding residues. Superposition of the backbone heavy atoms (N, C ^{α} , and C[']) of the final ensemble of 20 Vc1.2 structures with those of Vc1.1 (30) gave average group root-mean-square deviation values of 0.66 Å, a value no larger than the root-mean-square deviation within the Vc1.2 family, indicating that the backbone structures are highly conserved in these α -conotoxins. Therefore, the different subtype specificities of Vc1.2 and Vc1.1 for nAChR binding must arise from the specific amino acid side chain differences in these toxins. Amino acid residues affecting the affinity of Vc1.1 for the $\alpha 9\alpha 10$ subtype were determined by scanning mutagenesis (54). Vc1.2 differs from Vc1.1 in only four of those residues (Asp⁵, Arg⁷, Asp¹¹, and His¹², see Figs. 4C and 5). Based on high sequence similarities between Vc1.2 and Vc1.3, it is anticipated that the two embryonic toxins share the same structure. The additional Pro⁷ in Vc1.3 is unlikely to affect the α -helical structure as demonstrated by comparing the solution structure of Vc1.2 with that of PnIA, an α -conotoxin with Pro⁶ and Pro⁷ in the first loop (supplemental Fig. 3). Therefore, differences in their ability to mediate GABA_B receptor/N-type Ca²⁺ channel inhibition are likely to arise from specific side chain differences (Pro⁷, Ile⁹, Ala¹⁰, and Leu¹⁵ in Vc1.3, see Fig. 5). Likewise, Vc1.3 differs from Vc1.2 in only three side chains important for $\alpha 3\beta 2$ and $\alpha 7$ binding (Asn⁵, Ile⁹, and Leu¹⁵ in Vc1.3 (51, 55)) indicating that changes in these side chains may abolish binding to these nAChR subtypes (Fig. 5).

Comparative Anatomy of the Embryonic and Adult Foregut—Regions of the foregut important for venom biosynthesis, transport, and delivery were identified in adult specimens of *C. victoriae* (Fig. 6A). The venom apparatus consists of a long convoluted venom duct for toxin biosynthesis, a muscular venom bulb believed to be involved in venom transport (56), and harpoon-like radula teeth responsible for injecting the venom into the prey (Fig. 6, A and C) (57). Toxin biosynthesis and potential post-translational modifications take place in the columnar epithelial layer of the venom duct (58). Following biosynthesis, the venom is packed into ovoid-shaped granules that are densely packed into larger circular vesicles upon secretion from the epithelial cells (58). Histological examination of the em-

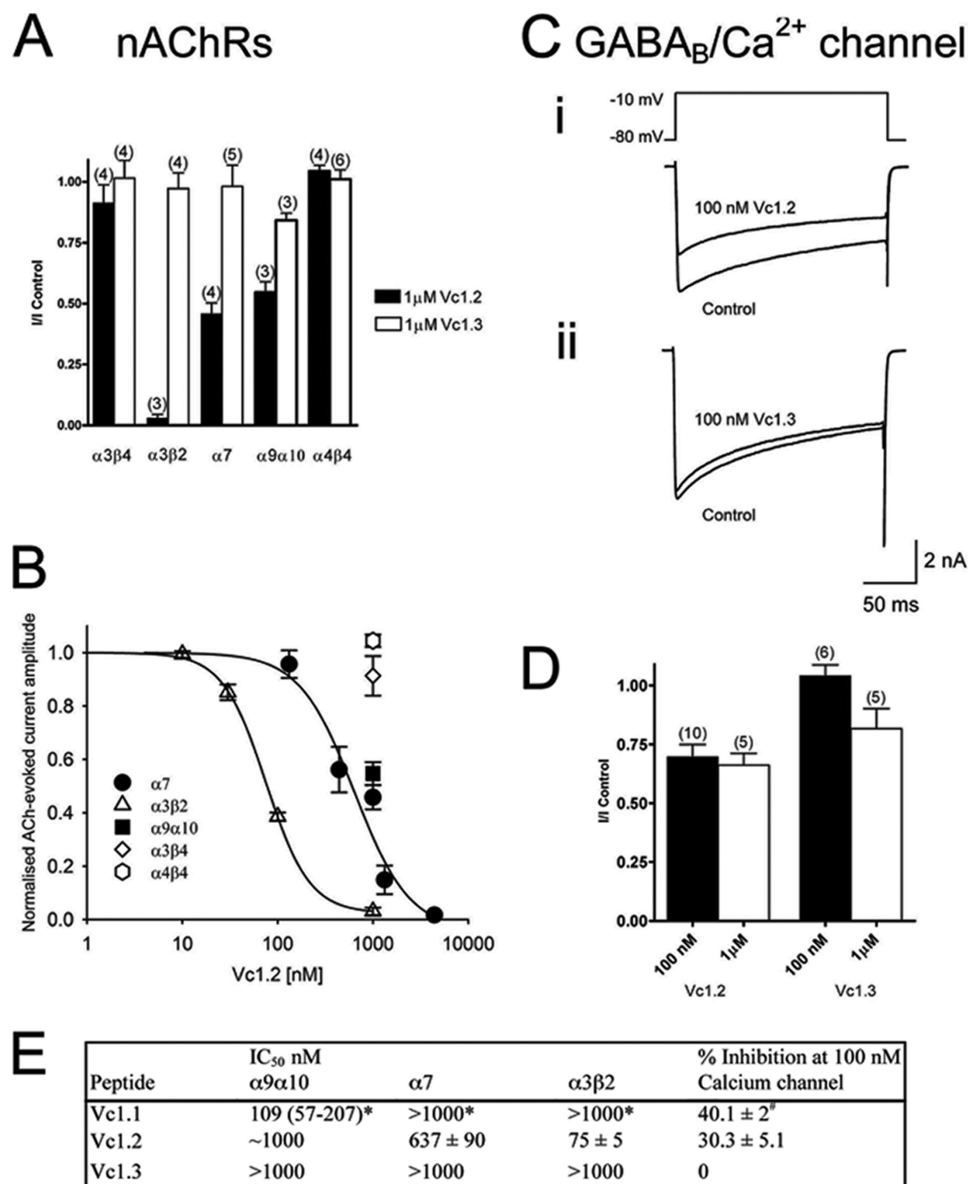


FIGURE 3. Vc1.2 and Vc1.3 inhibition of nAChRs expressed in *Xenopus* oocytes and Ca²⁺ channel currents in rat DRG neurons. *A*, bar graph of the relative inhibition of nAChRs expressed in *Xenopus* oocytes by 1 μM Vc1.2 and Vc1.3. Vc1.2 (1 μM) completely inhibited α3β2 nAChRs and inhibited α7 and α9α10 by 54 and 45%, respectively. Vc1.3 was inactive at all neuronal nAChR subtypes. *B*, concentration-response curves obtained for Vc1.2 inhibition of nAChR subtypes. Vc1.2 was most active at α3β2 nAChRs with an IC₅₀ of 75 ± 5 nM (▲; *n* = 3), 637 ± 90 nM for α7 (●; *n* = 4–6), and ~1 μM for α9α10 (■; *n* = 3). *C*, superimposed depolarization-activated whole-cell Ba²⁺ currents elicited by voltage steps from a holding potential of –80 to –10 mV in the absence (control) and presence of 100 nM Vc1.2 (*panel i*) and 100 nM Vc1.3 (*panel ii*), respectively. *D*, bar graph of the relative inhibition of HVA Ca²⁺ channel currents in rat DRG neurons by 100 nM and 1 μM Vc1.2 and Vc1.3. *E*, comparison of the IC₅₀ values of Vc1.1, Vc1.2, and Vc1.3 at different nAChR subtypes and percentage inhibition of calcium currents in isolated DRG neurons. Values determined in this study represent mean ± S.E. * indicates mean plus 95% confidence interval (54), and # represents mean ± S.E. (24).

bryos revealed that at the time when embryos of *C. victoriae* were sampled and fixed for sectioning, they did not possess the characteristic features of a functional venom apparatus. Although the radula sac could be resolved in histological sections (Fig. 6*B*, *panel iv*), the proboscis and venom duct were not yet differentiated. The venom duct in *Conus* is believed to develop from an outpocketing of the mid-esophageal wall (15); however, this differentiation could not be observed in any of the embryonic specimens examined.

Mass Spectrometric Analysis of Venom Peptide Preparations—Liquid chromatography coupled with mass spectrometry (LC/MS) revealed a complex composition of *C. victoriae* venom

(supplemental Fig. 4*A*). Although the presence of multiple analogues of Vc1.1 containing hydroxyproline and/or γ-carboxyglutamate was confirmed in this complex mixture (supplemental Fig. 4*B* (45, 59)), novel embryonic α-conotoxins were not detected in the adult's venom despite extensive and targeted LC-MS/MS analysis for various candidate venom peptide precursors. This finding indicates that although adults express embryonic toxin mRNAs, minimal or no translation into bioactive peptides takes place. Alternatively, the translated peptides may have been present in the venom but could not be detected using LC/MS due to unanticipated post-translational modifications. Analyses of LC/MS data obtained for *C. victoriae*

TABLE 1
Structural statistics for Vc1.2

No. of distance constraints	202
Intra-residue ($i = j$)	105
Sequential ($ i - j = 1$)	67
Short ($1 < i - j < 6$)	29
Long	1
No. of dihedral constraints	16
Energy (kcal/mol)^a	
E_{NOE}	4.1 ± 0.6
Deviations from ideal geometry^b	
Bonds	$0.0038 \pm 0.0002 \text{ \AA}$
Angles	$0.6980 \pm 0.0184^\circ$
Impropers	$0.5730 \pm 0.0273^\circ$
Mean global R.M.S.D. (\AA)^c	
Backbone heavy atoms (N, Ca, C')	0.66 ± 0.19
All heavy atoms	1.02 ± 0.21
Ramachandran plot^d	
Most favored	89.6%
Allowed	10.4%
Additionally allowed	0%
Disallowed	0%

^a The values for E_{NOE} are calculated from a square well potential with force constants of $50 \text{ kcal mol}^{-1} \text{ \AA}^2$.

^b The values for the bonds, angles, and impropers show the deviations from ideal values based on perfect stereochemistry.

^c Mean pairwise root-mean-square deviation (R.M.S.D.) over all residues calculated in MOLMOL.

^d Data are as determined by the program PROCHECK-NMR for all residues except Gly and Pro.

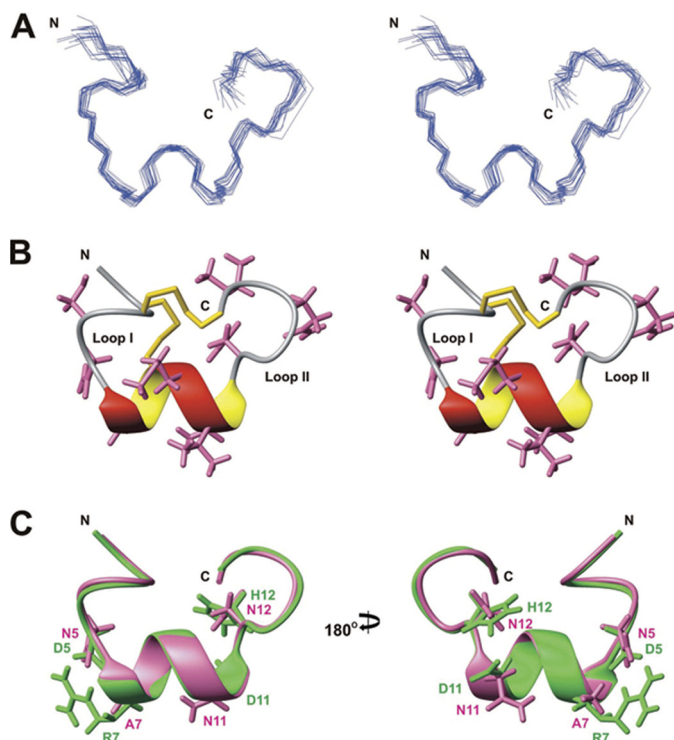


FIGURE 4. Solution structure of Vc1.2. *A*, stereo view of the family of 20 final structures of Vc1.2, superimposed over the backbone heavy atoms. *B*, stereo ribbon view of the closest-to-average structure of Vc1.2 highlighting the α -helix and two disulfide bonds. Side chains are shown except for prolines. *C*, comparison of the solution structures of Vc1.2 (pink) and Vc1.1 (30) (Protein Data Bank code 2H8S, green). Structures are superimposed over the backbone heavy atoms. Side chains of Vc1.1 residues important for $\alpha 9\alpha 10$ nAChR binding (30) and equivalent residues in Vc1.2 are shown.

venom anticipated disulfide bond formation, C-terminal amidation, hydroxylation of prolines, and γ -carboxylation of glutamate as well as differential C- and N-terminal cleavage. Electrospray ionization-MS/MS on the hybrid quadrupole-TOF



FIGURE 5. Alignment of α -conotoxins from *C. victoriae* highlighting residues important for biological function. Differences in sequence between the embryonic toxins Vc1.2 and Vc1.3 to the adult toxin Vc1.1 are shown in green. Amino acid residues likely to have caused a loss in activity toward the $\alpha 9\alpha 10$ neuronal nicotinic subtype (54), the N-type calcium channels,³ and the $\alpha 7$ subtype (55) are highlighted in pink and yellow and depicted with a frame, respectively. The disulfide bonds between Cys¹-Cys³ and Cys²-Cys⁴ are indicated by black lines. The backbone loops formed by this disulfide connectivity are shown below the sequences. All three C termini are likely to be amidated (#), a common modification in conotoxins.

mass spectrometer (QSTAR Elite, AB SCIEX) is highly sensitive allowing for the detection of peptides in the sub-femtomole range. Thus, failure to identify Vc1.2 and Vc1.3 in the venom of *C. victoriae* is unlikely to reflect the sensitivity of the detection method used.

DISCUSSION

Molecular sequencing revealed venom mRNA expression in embryos of *C. victoriae* and led to the identification of five novel O- and two α -conotoxin transcripts as well as confirmed the presence of mRNA encoding Vc1.1, a pharmacologically active peptide identified previously in adult specimens of *C. victoriae* (43). Thus, targeting different developmental stages proved to be a powerful technique for the discovery of novel bioactive peptides that are masked in the adult by the presence of highly abundant transcripts. Testing the embryonic α -conotoxins against different subtypes of the neuronal nicotinic receptor revealed that the embryonic toxin peptides had different target specificities. The embryonic peptide Vc1.2 exhibited high affinity toward the $\alpha 3\beta 2$ and $\alpha 7$ nAChR subtype but lower activity toward $\alpha 9\alpha 10$, the preferred receptor subtype for Vc1.1 (52).

Little is known about the presence or distribution of the nAChRs in invertebrates (60). In mammals, the $\alpha 7$ subtype is among the most abundant nicotinic receptors (61). With an unusually high permeability for calcium ions, this subtype regulates many calcium-dependent events throughout the central and peripheral nervous system (61). In contrast, in mice, the expression of the $\alpha 3\beta 2$ subtype is restricted to the habenulo-interrupted tract in the brain (62). Similarly, expression of the $\alpha 9\alpha 10$ nicotinic receptor is restricted to the cochlear hair cells, peripheral blood lymphocytes (63), skin keratinocytes (64, 65), and dorsal root ganglia (66, 67) where co-expression with $\alpha 7$ has been observed (68). Given this subtype-specific expression pattern of the nAChRs, conotoxins that selectively antagonize different nicotinic subtypes are likely to exhibit distinct biological functions.

The structures of Vc1.1 and Vc1.2 were almost identical, and changes in their target specificity were mediated by substitutions of a small number of amino acid side chains, although the disulfide scaffold was conserved (25, 55). This extraordinary ability to generate peptides with novel neuronal activities but equal structural stability has enabled cone snails to quickly adapt to changes in their biotic environment and rapidly diversify. Combining our findings on the structure-activity relation-

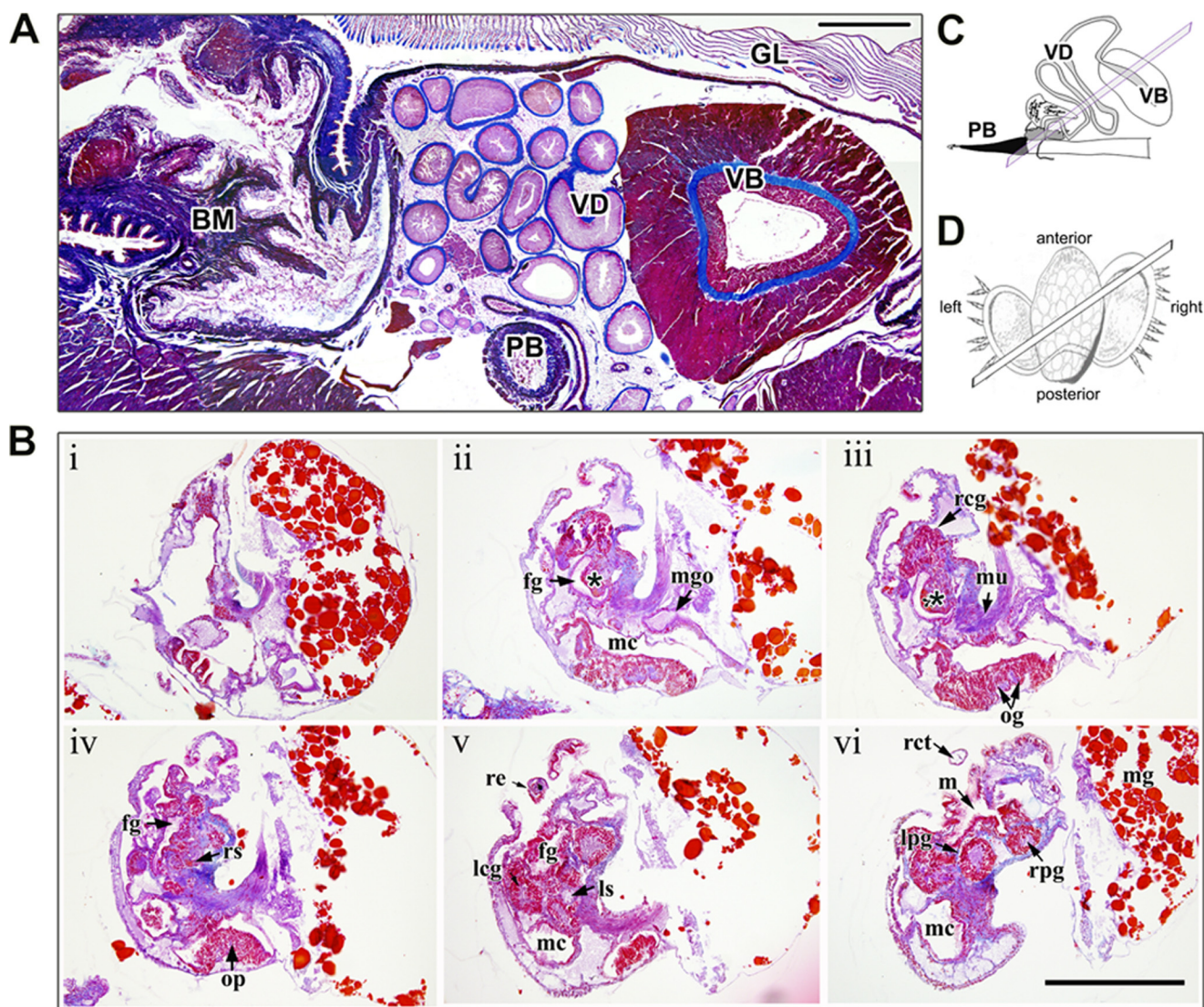


FIGURE 6. **Histological preparations of the adult venom apparatus and embryos of *C. victoriae*.** Sections were Mallory-stained and cut at 7 μm thickness. *A*, cross-section through the venom apparatus of *C. victoriae* showing the venom duct (VD), the venom bulb (VB), the proboscis (PB), the gill (GL), and the buccal mass (BM). Scale bar, 200 μm . *B*, serial sections (panels i–vi) through an embryo depicting foregut (fg), left cerebral ganglion (lcg), left pedal ganglion (lpg), left statocyst (ls), mouth (m), mantle cavity (mc), midgut (mg), midgut opening (mgo), muscle (mu), osphradial ganglia (og), osphradium (op), right cerebral ganglion (rcg), right cephalic tent (rct), right eye (re), radula sack (rs), right pedal ganglion (rpg), style sac (ss). The incipient venom gland is marked with an asterisk. Scale bar, 200 μm . *C*, schematic of the venom apparatus showing orientation of section shown in *A*. *D*, drawing of the larvae showing orientation of serial sections shown in *B*.

ships of Vc1.2 and Vc1.3 with data obtained from scanning mutagenesis studies on Vc1.1 (54),⁵ residues causing a shift in target specificity can now be predicted. Amino acid substitutions affecting Asp⁵ to Arg⁷ and Asp¹¹ to Ile¹⁵ caused a significant decrease in the affinity of Vc1.1 toward the $\alpha 9\alpha 10$ subtype (54). Because only four of these amino acids differ between Vc1.1 and Vc1.2, substitutions of one or more of these residues are likely to have caused the shift in subtype specificity. Interestingly, in Vc1.1, three of these side chains are charged, and one is an imidazolium ring. In Vc1.2, all are replaced by uncharged residues. This charge loss may contribute to the decreased affinity of Vc1.2 for the $\alpha 9\alpha 10$ subtype. Unlike Vc1.1 and Vc1.2, Vc1.3 did not inhibit GABA_B receptor/N-type Ca²⁺ channels. Vc1.3 differs from the other two peptides in five posi-

tions, four of which are known to be important sites for GABA_B receptor recognition.⁵ Likewise, specific differences in amino acids between Vc1.3 and Vc1.2 must contribute to a loss in activity toward the $\alpha 3\beta 2$ and $\alpha 7$ subtypes (51, 55).

This poses the following questions. Why do these toxins have a different biological target than the most abundant α -conotoxin in the adult snail? Why do cone snail embryos express toxin-encoding mRNAs in the first place? Histological investigations demonstrated that at the time of sampling, the cells of the mid-esophagus had not yet formed the esophageal ventral groove that will later develop into the venom gland. However, it is possible that the cells of the incipient venom gland had begun to hypertrophy and produce mRNA transcripts of toxin genes prior to tissue differentiation. Embryos were harvested approximately 2 weeks before hatching occurred. Unfortunately, hatched stages could not be recovered. Morphological

⁵ D. J. Adams and B. Callaghan, unpublished data.

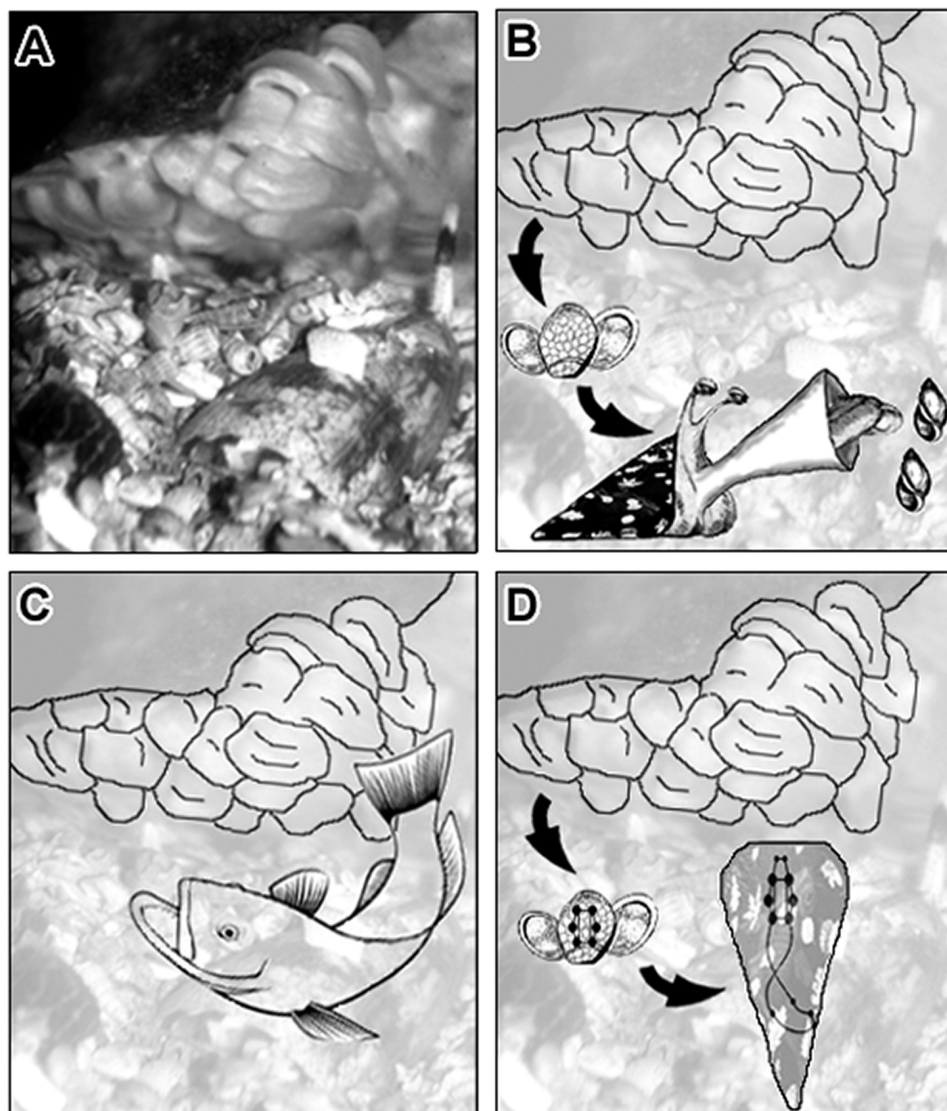


FIGURE 7. **Potential usage of toxins in cone snail embryos.** A, *C. victoriae* guarding egg capsules. Cone snail embryos may express toxin mRNA transcripts as preparation for a predatory life style (B) or to deter predators (C), or toxin peptides may be involved in other biological pathways such as neuronal signaling (D).

studies of embryos of *Conus anemone* showed that immediately prior to hatching the esophageal diverticulum was filled with secretory granules (15) likely to contain conotoxins (58). Oocytes of some marine organisms such as sea urchins and starfish store maternal mRNAs enabling rapid biosynthesis of vital proteins in the developing embryo (69–71). Given that *C. anemone* embryos synthesize venom granules in the incipient venom duct tissue, toxin mRNA transcripts identified in *C. victoriae* embryos are not likely to be of maternal origin.

Although we were unable to detect transcripts at the protein level, it is unlikely that the embryonic toxins solely represent silent transcripts. Electrophysiological investigations demonstrated that the embryonic toxin Vc1.2 is active in its mature state and combined with the presence of a variety of different O-superfamily toxins, it indicates that embryos express functionally active peptides.

Juveniles of *C. pennaceus* and *Conus mediterraneus* have been reported to feed on small gastropods shortly after hatching (17, 72). Based on these findings, venom mRNA expression

in cone snail embryos could represent preparation of the venom machinery for a predatory lifestyle (Fig. 7B). *C. victoriae* is therefore likely to hatch from the egg capsule as a short lived nonfeeding larva or a juvenile. Similarly, mRNA encoding chymotrypsin-like preproprotease, a highly expressed protein in the intestine of the adult gastropod *Halotis rufescens*, was detected in amebocyte of the digestive tissue of embryos well before metamorphosis and gut morphogenesis (73). When the relationship between the morphogenesis and appearance of secretory components were studied in embryos of the viper *Vipera palaestinae*, neurotoxins and venom-specific enzymes were detected by immunohistochemistry together with secretion of granules into the lumen of the venom gland days before hatching (74). As proposed for cone snails, it can be hypothesized that snake embryos synthesize venom to prime for a predatory lifestyle. Juveniles of *C. magus* experienced an age-related change in prey type from polychaetes to fish (19). It is now well understood that the venom composition of fish-hunting cone snails is different from that of mollusc and worm hunters (2).

Embryonic Toxin Expression in Marine Cone Snails

Adult *C. victoriae* are molluscivorous (mollusc-eating). The feeding behavior of juvenile *C. victoriae* has not been investigated, but differences in toxin expression between the embryos and the adults may indicate that similar lifestyle changes occur in *C. victoriae*. Differences in the relative abundances of conotoxins may therefore indicate that the venom composition undergoes ontogenetic changes as observed in other venomous animals (75). Behavioral studies on newly hatched juveniles and investigations on relative abundances of conotoxins at different developmental stages are needed to further support this notion.

Cone snail embryos and newly hatched juveniles may synthesize venom for defense rather than predation (Fig. 7C). Injection of the venom into the snail's prey causes immediate paralysis (76), and thus compounds that are utilized for hunting can also serve for defense. Anecdotal evidence for the usage of venom in defense by adult cone snails is emerging (11). Synthesis of defensive or deterrent compounds is a common phenomenon in embryos and larvae of many marine organisms (77–80). Defensive compounds include glycosides (79), alkaloids (81), cyclic peptides (82), halogenated phenols (80), and terpenes (77). Interestingly, comparisons between adult and larval deterrent profiles revealed that the same compounds are utilized by different life stages, but concentrations can vary extensively (78, 80, 82). In cone snails, full development of the venom apparatus occurs during or shortly after hatching (16, 17, 72). It can be hypothesized that juveniles of *C. victoriae* inject the novel embryonic toxins into their prey and potential predators/competitors. Consequently, changes in the venom repertoire may reflect differences in the type of predators and competitors with which these animals interact.

It is now well understood that most toxins are proteins that have originally been recruited from ancestral body proteins through gene duplication and subsequent mutation and/or deletion events (83). The three-dimensional scaffold of the newly generated toxin multigene family is generally preserved, although the remaining residues diversify to generate molecules with novel biological activities (83). For example, the snake three-finger neurotoxins are derivations of endogenous neuropeptides similar to a family of proteins found in humans, the SLUR proteins (84). SLUR proteins therefore belong to a group of toxin-like proteins with nontoxic endogenous activities. For example, SLURP-1 is a disulfide-rich endogenous ligand of the $\alpha 7$ nicotinic receptor subtype (85) and is expressed in a variety of different tissue types, including skin, gums, stomach, and the esophagus (86). The bee ω -conotoxin-like protein 1 (OCLP1) is another example of a toxin-like peptide that potentially represents an ancestral toxin protein (87). OCLP1 exhibits the characteristic disulfide scaffold of cone snail ω -conotoxins and is highly expressed in the bee brain where it has been suggested to modulate voltage-gated Ca^{2+} channel activity (87).

As whole embryos were taken for molecular sequencing, toxin transcripts might have originated from tissues other than the incipient venom gland. The embryonic peptides could therefore represent toxin-like compounds that function as endogenous neuronal modulators in the developing snail embryo (Fig. 7D). Sequencing and phylogenetic analysis of toxins and toxin-like peptides from the venom gland and tissues not involved in venom biosynthesis could be revealing in this context.

In summary, this study has identified novel α - and O-toxin peptides in embryos of the cone snail *C. victoriae*. Embryonic α -conotoxins differ significantly in their biological function from the most abundant α -conotoxin in the adult, although the three-dimensional structure is conserved. We suggest that the venom of cone snails undergoes ontogenetic variations and that the early onset of venom expression in embryos most likely represents preparation for predation and/or defense, although a role in endogenous processes cannot be ruled out. Future analyses of embryos from additional mating events will be informative in this context. Behavioral studies and further characterization of the venom composition in embryos and adult snails will provide insights into the mechanisms underlying the generation of biodiversity in *Conus*.

Acknowledgments—We thank Bruce Abaloz and Dr. Neil Young for help with histological preparation, Dr. Bruce Livett for reviewing the manuscript, John Ahern for the maintenance of specimens, and Dr. Robyn Bradbury and Johan Paz for assistance in collection of specimens.

Note Added in Proof—Since our manuscript was accepted, we have learned of some earlier studies that have shown embryonic toxin expression in sea anemones (88, 89) and Hydra embryos (90).

REFERENCES

1. Terlau, H., and Olivera, B. M. (2004) *Physiol. Rev.* **84**, 41–68
2. Olivera, B. M. (2006) *J. Biol. Chem.* **281**, 31173–31177
3. Norton, R. S., and Olivera, B. M. (2006) *Toxicon* **48**, 780–798
4. Pisarewicz, K., Mora, D., Pflueger, F. C., Fields, G. B., and Mari, F. (2005) *J. Am. Chem. Soc.* **127**, 6207–6215
5. Lopez-Vera, E., Walewska, A., Skalicky, J. J., Olivera, B. M., and Bulaj, G. (2008) *Biochemistry* **47**, 1741–1751
6. Craig, A. G., Park, M., Fischer, W. H., Kang, J., Compain, P., and Piller, F. (2001) *Toxicon* **39**, 809–815
7. Loughnan, M. L., Nicke, A., Jones, A., Adams, D. J., Alewood, P. F., and Lewis, R. J. (2004) *J. Med. Chem.* **47**, 1234–1241
8. Jakubowski, J. A., Kelley, W. P., Sweedler, J. V., Gilly, W. F., and Schulz, J. R. (2005) *J. Exp. Biol.* **208**, 2873–2883
9. Davis, J. M., Boswell, B. A., and Bächinger, H. P. (1989) *J. Biol. Chem.* **264**, 8956–8962
10. Jones, A., Bingham, J. P., Gehrmann, J., Bond, T., Loughnan, M., Atkins, A., Lewis, R. J., and Alewood, P. F. (1996) *Rapid Commun. Mass Spectrom.* **10**, 138–143
11. Olivera, B. M. (2002) *Annu. Rev. Ecol. System* **33**, 25–47
12. Cummins, S. F., Nuurai, P., Nagle, G. T., and Degnan, B. M. (2010) *Peptides* **31**, 394–401
13. Vreugdenhil, E., Jackson, J. F., Bouwmeester, T., Smit, A. B., Van Minnen, J., Van Heerikhuizen, H., Klootwijk, J., and Joosse, J. (1988) *J. Neurosci.* **8**, 4184–4191
14. Kohn, A. J., and Perron, F. E. (1994) *J. Marine Biol. Assoc. UK.* **74**, 744
15. Ball, A. D. (2002) *Bolletino. Malacologico.* **38**, 51–78
16. Ball, A. D. (1999) in *The Seagrass Flora and Fauna of Rottnest Island, Western Australia* (Wells, D. I., and Wells, F. E., eds) pp. 137–162, Western Australian Museum, Perth, Western Australian
17. Perron, F. E. (1981) *Mar. Biol.* **61**, 215–220
18. Perron, F. E. (1980) *J. Exp. Marine Biol. Ecol.* **42**, 27–38
19. Nybakken, J., and Perron, F. E. (1988) *Mar. Biol.* **98**, 239–242
20. Cartier, G. E., Yoshikami, D., Gray, W. R., Luo, S., Olivera, B. M., and McIntosh, J. M. (1996) *J. Biol. Chem.* **271**, 7522–7528
21. Loughnan, M., Bond, T., Atkins, A., Cuevas, J., Adams, D. J., Broxton, N. M., Livett, B. G., Down, J. G., Jones, A., Alewood, P. F., and Lewis, R. J. (1998) *J. Biol. Chem.* **273**, 15667–15674
22. Johnson, D. S., Martinez, J., Elgoyhen, A. B., Heinemann, S. F., and McIntosh, J. M. (1995) *Mol. Pharmacol.* **48**, 194–199

23. Callaghan, B., and Adams, D. J. (2010) *Channels* **4**, 51–54
24. Callaghan, B., Haythornthwaite, A., Berecki, G., Clark, R. J., Craik, D. J., and Adams, D. J. (2008) *J. Neurosci.* **28**, 10943–10951
25. Whiteaker, P., Christensen, S., Yoshikami, D., Dowell, C., Watkins, M., Gulyas, J., Rivier, J., Olivera, B. M., and McIntosh, J. M. (2007) *Biochemistry* **46**, 6628–6638
26. Pantin, C. F. (1946) *Notes on Microscopical Technique for Zoologists*, Cambridge University Press, Cambridge
27. Safavi-Hemami, H., Bulaj, G., Olivera, B. M., Williamson, N. A., and Purcell, A. W. (2010) *J. Biol. Chem.* **285**, 12735–12746
28. Katoh, K., Kuma, K., Toh, H., and Miyata, T. (2005) *Nucleic Acids Res.* **20**, 511–518
29. Emanuelsson, O., Brunak, S., von Heijne, G., and Nielsen, H. (2007) *Nat. Protoc.* **2**, 953–971
30. Clark, R. J., Fischer, H., Nevin, S. T., Adams, D. J., and Craik, D. J. (2006) *J. Biol. Chem.* **281**, 23254–23263
31. Nevin, S. T., Clark, R. J., Klimis, H., Christie, M. J., Craik, D. J., and Adams, D. J. (2007) *Mol. Pharmacol.* **72**, 1406–1410
32. Bartels, C., Xia, T. H., Billeter, M., Guntert, P., and Wuthrich, K. (1995) *J. Biomol. NMR* **6**, 1–10
33. Güntert, P., Mumenthaler, C., and Wüthrich, K. (1997) *J. Mol. Biol.* **273**, 283–298
34. Herrmann, T., Güntert, P., and Wüthrich, K. (2002) *J. Mol. Biol.* **319**, 209–227
35. Shen, Y., Delaglio, F., Cornilescu, G., and Bax, A. (2009) *J. Biomol. NMR* **44**, 213–223
36. Schwieters, C. D., Kuszewski, J. J., Tjandra, N., and Clore, G. M. (2003) *J. Magn. Reson.* **160**, 65–73
37. Linge, J. P., Williams, M. A., Spronk, C. A., Bonvin, A. M., and Nilges, M. (2003) *Proteins* **50**, 496–506
38. Laskowski, R. A., Rullmann, J. A., MacArthur, M. W., Kaptein, R., and Thornton, J. M. (1996) *J. Biomol. NMR* **8**, 477–486
39. Koradi, R., Billeter, M., and Wuthrich, K. (1996) *J. Mol. Graph.* **14**, 51–55, 29–32
40. Seavey, B. R., Farr, E. A., Westler, W. M., and Markley, J. L. (1991) *J. Biomol. NMR* **1**, 217–236
41. López-Vera, E., Aguilar, M. B., Schiavon, E., Marinzi, C., Ortiz, E., Restano Cassulini, R., Batista, C. V., Possani, L. D., Heimer de la Cotera, E. P., Peri, F., Becerril, B., and Wanke, E. (2007) *FEBS J.* **274**, 3972–3985
42. Luo, S., Zhangsun, D., Zhang, B., Quan, Y., and Wu, Y. (2006) *J. Pept. Sci.* **12**, 693–704
43. Sandall, D. W., Satkunanathan, N., Keays, D. A., Polidano, M. A., Liping, X., Pham, V., Down, J. G., Khalil, Z., Livett, B. G., and Gayler, K. R. (2003) *Biochemistry* **42**, 6904–6911
44. Zhangsun, D., Luo, S., Wu, Y., Zhu, X., Hu, Y., and Xie, L. (2006) *Chem. Biol. Drug Des.* **68**, 256–265
45. Jakubowski, J. A., Keays, D. A., Kelley, W. P., Sandall, D. W., Bingham, J. P., Livett, B. G., Gayler, K. R., and Sweedler, J. V. (2004) *J. Mass Spectrom.* **39**, 548–557
46. Heinemann, S. H., and Leipold, E. (2007) *Cell. Mol. Life Sci.* **64**, 1329–1340
47. Halai, R., and Craik, D. J. (2009) *Nat. Prod. Rep.* **26**, 526–536
48. Gatton, M. L., Peters, J. M., Gresty, K., Fowler, E. V., Chen, N., and Cheng, Q. (2006) *Am. J. Trop. Med. Hyg.* **75**, 212–218
49. Stock, D. W., Buchanan, A. V., Zhao, Z., and Weiss, K. M. (1996) *Genomics* **37**, 234–237
50. Santos, A. D., McIntosh, J. M., Hillyard, D. R., Cruz, L. J., and Olivera, B. M. (2004) *J. Biol. Chem.* **279**, 17596–17606
51. Luo, S., Nguyen, T. A., Cartier, G. E., Olivera, B. M., Yoshikami, D., and McIntosh, J. M. (1999) *Biochemistry* **38**, 14542–14548
52. Vincler, M., Wittenauer, S., Parker, R., Ellison, M., Olivera, B. M., and McIntosh, J. M. (2006) *Proc. Natl. Acad. Sci. U.S.A.* **103**, 17880–17884
53. Hu, S. H., Gehrmann, J., Guddat, L. W., Alewood, P. F., Craik, D. J., and Martin, J. L. (1996) *Structure* **4**, 417–423
54. Halai, R., Clark, R. J., Nevin, S. T., Jensen, J. E., Adams, D. J., and Craik, D. J. (2009) *J. Biol. Chem.* **284**, 20275–20284
55. Millard, E. L., Daly, N. L., and Craik, D. J. (2004) *Eur. J. Biochem.* **27**, 2320–2326
56. Le Gall, F., Favreau, P., Richard, G., Letourneux, Y., and Molgó, J. (1999) *Toxicon* **37**, 985–998
57. Kohn, A. J., Nybakken, J. W., and Van Mol, J. J. (1972) *Science* **176**, 49–51
58. Marshall, J., Kelley, W. P., Rubakhin, S. S., Bingham, J. P., Sweedler, J. V., and Gilly, W. F. (2002) *Biol. Bull.* **203**, 27–41
59. Townsend, A., Livett, B. G., Bingham, J. P., Truong, H. T., Karas, J. A., O'Donnell, P., Williamson, N. A., Purcell, A. W., and Scanlon, D. (2009) *Int. J. Pept. Res. Ther.* **15**, 195–203
60. Jones, A. K., Brown, L. A., and Sattelle, D. B. (2007) *Invert. Neurosci.* **7**, 67–73
61. Sargent, P. B. (1993) *Annu. Rev. Neurosci.* **16**, 403–443
62. Drago, J., McColl, C. D., Horne, M. K., Finkelstein, D. I., and Ross, S. A. (2003) *Cell. Mol. Life Sci.* **60**, 1267–1280
63. Peng, H., Ferris, R. L., Matthews, T., Hiel, H., Lopez-Albaitero, A., and Lustig, L. R. (2004) *Life Sci.* **76**, 263–280
64. Kurzen, H., Berger, H., Jager, C., Hartschuh, W., and Maas-Szabowski, N. (2005) *Exp. Dermatol.* **14**, 155
65. Arredondo, J., Nguyen, V. T., Chernyavsky, A. I., Bercovich, D., Orr-Urtreger, A., Kummer, W., Lips, K., Vetter, D. E., and Grando, S. A. (2002) *J. Cell Biol.* **159**, 325–336
66. Haberberger, R. V., Bernardini, N., Kress, M., Hartmann, P., Lips, K. S., and Kummer, W. (2004) *Autonomic Neurosci.* **113**, 32–42
67. Lips, K. S., Pfeil, U., and Kummer, W. (2002) *Neuroscience* **115**, 1–5
68. Hone, A. J., Whiteaker, P., Christensen, S., Xiao, Y., Meyer, E. L., and McIntosh, J. M. (2009) *J. Neurochem.* **111**, 80–89
69. Brandhorst, B. P. (1985) *Dev. Biol.* **1**, 525–527
70. Nash, M. A., Kozak, S. E., Angerer, L. M., Angerer, R. C., Schatten, H., Schatten, G., and Marzluff, W. F. (1987) *J. Cell Biol.* **104**, 1133–1142
71. Howell, A. M., Cool, D., Hewitt, J., Ydenberg, B., Smith, M. J., and Honda, B. M. (1987) *J. Mol. Evol.* **25**, 29–36
72. Franc, A. (1943) *Faculty of Science*. Ph.D. thesis, pp. 1–158, University of Algeria
73. Degnan, B. M., Groppe, J. C., and Morse, D. E. (1995) *Roux's Arch. Dev. Biol.* **205**, 97–101
74. Fein, A., Bdolah, A., and Kochva, E. (1971) *Dev. Biol.* **24**, 520–532
75. Escoubas, P., Corzo, G., Whiteley, B. J., Célérier, M. L., and Nakajima, T. (2002) *Rapid Commun. Mass Spectrom.* **16**, 403–413
76. Olivera, B. M. (1997) *Mol. Biol. Cell.* **8**, 2101–2109
77. Coll, J. C., Leone, P. A., Bowden, B. F., Carroll, A. R., König, G. M., Heaton, A., de Nys, R., Maida, M., Aliño, P. M., Willis, R. H., Babcock, R. C., Florian, Z., Clayton, M. N., Miller, R. L., and Alderslade, P. N. (1995) *Mar. Biol.* **123**, 1432–1793
78. Slattery, M., Hines, G. A., Starmer, J., and Paul, V. J. (1999) *Coral Reefs* **18**, 75–84
79. Howden, M. E., Lucas, J., McDuff, M., and Salathe, R. (1974) in *Crown-of-Thorns Starfish: Seminar Proceedings, September 6, 1974*, Government Publishing Service, Canberra, Brisbane, Australia
80. Cowart, J. D., Fielman, K. T., Woodin, S. A., and Lincoln, D. E. (2000) *Mar. Biol.* **136**, 993–1002
81. Lindquist, N., and Fenical, W. (1991) *Experientia* **47**, 504–506
82. Lindquist, N., Hay, M. E., and Fenical, W. (1992) *Ecol. Monogr.* **62**, 547–568
83. Fry, B. G., Roelants, K., Champagne, D. E., Scheib, H., Tyndall, J. D., King, G. F., Nevalainen, T. J., Norman, J. A., Lewis, R. J., Norton, R. S., Renjifo, C., and de la Vega, R. C. (2009) *Annu. Rev. Genomics Hum. Genet.* **10**, 483–511
84. Fry, B. G. (2005) *Genome Res.* **15**, 403–420
85. Faghieh, R., Gfesser, G. A., and Gopalakrishnan, M. (2007) *Recent Pat. CNS Drug Discov.* **2**, 99–106
86. Mastrangeli, R., Donini, S., Kelton, C. A., He, C., Bressan, A., Milazzo, F., Ciolli, V., Borrelli, F., Martelli, F., Biffoni, M., Serlupi-Crescenzi, O., Serani, S., Micangeli, E., El Tayar, N., Vaccaro, R., Renda, T., Lisciani, R., Rossi, M., and Papoian, R. (2003) *Eur. J. Endocrinol.* **13**, 560–570
87. Kaplan, N., Morpurgo, N., and Linial, M. (2007) *J. Mol. Biol.* **369**, 553–566
88. Moran, Y., Weinberger, H., Reitzel, A. M., Sullivan, J. C., Kahn, R., Gordon, D., Finnerty, J. R., and Gurevitz, M. (2008) *J. Mol. Biol.* **380**, 437–434
89. Moran, Y., Weinberger, H., Lazarus, N., Gur, M., Kahn, R., Gordon, D., and Gurevitz, M. (2009) *J. Mol. Evol.* **69**, 115–124
90. Genikhovich, G., Kürn, U., Hemmrich, G., and Bosch, T. C. (2006) *Dev. Biol.* **289**, 466–481